Anomalous Quantum Hall Effect of Light in Bloch-Wave Modulated Photonic Crystals

Kejie Fang[1,2,*] and Yunkai Wang[2,3]
[1]Department of Electrical and Computer Engineering, University of Illinois at Urbana-Champaign, Urbana, Illinois 61801, USA
[2]Micro and Nanotechnology Laboratory, University of Illinois at Urbana-Champaign, Urbana, Illinois 61801, USA
[3]Department of Physics, University of Illinois at Urbana-Champaign, Urbana, Illinois 61801, USA

(Received 5 February 2019; published 14 June 2019)

Effective magnetic fields have enabled unprecedented manipulation of neutral particles including photons. In most studied cases, the effective gauge fields are defined through the phase of mode coupling between spatially discrete elements, such as optical resonators and waveguides in the case for photons. Here, in the paradigm of Bloch-wave modulated photonic crystals, we show the creation of effective magnetic fields for photons in conventional dielectric continua for the first time, via Floquet band engineering. By controlling the phase and wave vector of Bloch waves, we demonstrated the anomalous quantum Hall effect for light with distinct topological band features due to delocalized wave interference. Based on a cavity-free architecture, in which Bloch-wave modulations can be enhanced using guided resonances in photonic crystals, the study here opens the door to the realization of effective magnetic fields at large scales for optical beam steering and topological light-matter phases with broken time-reversal symmetry.

DOI: 10.1103/PhysRevLett.122.233904

Photons, being charge neutral, are not susceptible to magnetic fields. Recently, several methods have been proposed to create effective magnetic fields for photons, including chiral mode coupling [1] and dynamic index modulation [2], leading to topological photonic states [3,4] and nonreciprocal light propagation [5,6]. In the scheme of dynamic index modulation, the effective gauge field is equivalent to the phase of a point modulation that is exerted to mediate the coupling between two spatially localized optical resonators with different frequencies [2]. Such a revelation enables analogies between modulated optical resonator lattices and condensed matter systems under magnetic fields via commonly used tight-binding models, but it nonetheless imposes challenges for experimental realization and practical uses. However, it is unknown how to create effective magnetic fields for photons in a continuum of conventional dielectrics, where electromagnetic fields are delocalized, invalidating the notion of local phase of mode coupling for effective gauge fields. Here, we study a new paradigm of dynamically modulated continua, which are photonic crystals subject to Bloch-wave modulations, in which spatial gauge fields for photons are revealed via Floquet band engineering [7,8]. In this approach, the continuum modulation induces static-band hybridization, leading to an equation of motion for electromagnetic waves that resembles that of charged particles under magnetic fields.

The paradigm of modulated electromagnetic continuum not only extends the concept of effective magnetic fields for photons to a largely unexplored yet experimentally accessible regime, but it also leads to topological photonic effects that have not been demonstrated before. As we will show, by selecting the wave vectors of Bloch-wave modulations, the net effective magnetic flux through the unit cell of photonic crystals vanishes. Nevertheless, the Floquet bands can still attain nonzero Chern numbers in the presence of time-reversal symmetry breaking caused by the dynamic modulation. This result represents the first anomalous quantum Hall effect for light in Floquet engineered photonic systems.

Here, we developed a first-principles based formalism along with *ab initio* simulations to reveal unique topological band features in Bloch-wave modulated photonic crystals due to delocalized wave interference. We also propose to use guided resonances or bound states in the continuum [9–11] to enhance the strength of Bloch-wave modulations that can be readily implemented with highly transducing optical or acoustic pump fields [12,13]. As a result, the proposed paradigm of a modulated continuum here opens the door to large-scale realization of effective magnetic fields for photons in normal dielectrics for new types of beam steering, dynamic signal processing, and topological states with broken time-reversal symmetry, which are highly tunable and reconfigurable via controlling the parameters of Bloch waves.

To study photonic crystals under continuum modulations, we start from Maxwell's equation with isotropic and temporally periodic permittivity $\epsilon(\mathbf{r},t)=\epsilon(\mathbf{r})+\delta(\mathbf{r},t)$:

$$i\frac{\partial}{\partial t}\begin{pmatrix}\epsilon(\mathbf{r},t)\mathbf{E}\\ \mathbf{H}\end{pmatrix}=\begin{pmatrix}& i\nabla\times\\ -i\nabla\times &\end{pmatrix}\begin{pmatrix}\mathbf{E}\\ \mathbf{H}\end{pmatrix}. \quad (1)$$

Here, $\epsilon(\mathbf{r})$ is the spatially periodic permittivity that defines the static photonic crystal, and $\delta(\mathbf{r},t)=\delta(\mathbf{r})\cos[\omega t+\phi(\mathbf{r})]$ is the temporal modulation of the permittivity with the

frequency ω, amplitude $\delta(\mathbf{r})$, and phase $\phi(\mathbf{r})$: all of which are real. Note that this form represents the most general monochromatic modulations. We have set $\epsilon_0 = \mu_0 = 1$ and $\mu = 1$ as for most dielectric materials at optical frequencies. Because of the time periodicity of the permittivity, according to the Floquet theorem [14], the eigenmodes of Eq. (1) can be found by decomposition of the fields into harmonics of the modulation frequency, i.e.,

$$(\mathbf{E} \quad \mathbf{H})^T \equiv \Psi = \sum_{n=-\infty}^{\infty} \psi_n e^{-i\chi t + in\omega t},$$

where χ is the quasifrequency [15]. We coin the resulting time-independent eigenmode equation the Floquet-Maxwell equation.

When the modulation has the form of Bloch waves [i.e., $\delta(\mathbf{r})e^{i\phi(\mathbf{r})} = u(\mathbf{r})e^{i\mathbf{q}\cdot\mathbf{r}}$] and $u(\mathbf{r})$ is a periodic function [note that $\phi(\mathbf{r})$ needs not be $\mathbf{q}\cdot\mathbf{r}$], we call such a modulated dielectric structure the Floquet photonic crystal. If the periodicities of $u(\mathbf{r})$ and the static photonic crystal are commensurable, then by applying a gauge transformation $U_{\text{gauge}}: \psi_n \to e^{in\mathbf{q}\cdot\mathbf{r}}\psi_n$, the Floquet-Maxwell equation becomes spatially periodic; thus, the eigenvalue χ can be labeled by a Bloch-wave vector $\mathbf{k}$, forming the Floquet band structure [15]. According to this formalism, the generation of the Floquet band structure, to the leading order, can be intuitively understood as the result of modulation induced static-band hybridization after frequency and momentum shift of the bands by ω and $\mathbf{q}$, respectively. Because of the nonvanishing momentum of the modulation, the Floquet band structure, with infinitely repeated branches (i.e., $\chi + n\omega$, $\forall\, n$, is also a solution of the Floquet-Maxwell equation), has the property $\chi(\mathbf{k}+\mathbf{q}) = \chi(\mathbf{k}) - \omega$.

With a spatially varying modulation phase $\phi(\mathbf{r})$, time-reversal symmetry in modulated photonic crystals is explicitly broken because the modulated permittivity is not invariant under time reversal $t \to -t$ for arbitrary positions. We use Floquet band engineering (i.e., modulation induced static-band coupling) to derive an effective gauge field for photons. For this purpose, we consider two static bands under dynamic modulations with a frequency close to the band gap that is larger than the bandwidth of each band. In this case, one can write down an approximate coupled-band equation resulted from the Floquet-Maxwell equation,

$$\frac{\partial^2 \mathbf{H}_1}{\partial t^2} = -\nabla \times \frac{1}{\epsilon}\nabla \times \mathbf{H}_1 + \nabla \times \frac{\delta}{\epsilon^2} e^{i\phi}\nabla \times \mathbf{H}_2, \quad (2)$$

$$\frac{\partial^2 \mathbf{H}_2}{\partial t^2} = -\nabla \times \frac{1}{\epsilon}\nabla \times \mathbf{H}_2 + \nabla \times \frac{\delta}{\epsilon^2} e^{-i\phi}\nabla \times \mathbf{H}_1, \quad (3)$$

where $\mathbf{H}_{1,2}$ are the magnetizing fields associated with the two bands. The effective gauge field for photons can be identified by comparing the equation of motion for the electromagnetic fields of one band with the Hamiltonian of charged particles in the presence of gauge fields, i.e., $\hat{H} = (-i\nabla - q\mathbf{A})^2/2m$, where the gauge field is the imaginary coefficient of the term that is linear in $\nabla(\cdot)$. Using this method, we find

$$\mathbf{A}_{\text{eff}}(\mathbf{r}) = \frac{1}{\omega^2}\text{Im}\left\{\nabla \cdot \left(\frac{\delta}{\epsilon^2} e^{i\phi}\nabla\left(\nabla \frac{\delta}{\epsilon^2} e^{-i\phi}\right)\right)\right\} \quad (4)$$

for transverse electric modes (the $\cdot$ represents the scalar product between the first ∇ and the last ∇) and

$$\mathbf{A}_{\text{eff}}(\mathbf{r}) = \frac{2}{\omega^2}\text{Im}\left\{\nabla^2\left(\frac{\delta}{\epsilon^2} e^{i\phi}\nabla \frac{\delta}{\epsilon^2} e^{-i\phi}\right)\right\} \quad (5)$$

for transverse magnetic (TM) modes in two-dimensional photonic crystals, respectively [15].

From Eqs. (4) and (5), it is remarkable that the effective gauge field is largely determined by the modulation phase, which is similar to the case of discretely modulated resonator lattices [2]; it is zero if $\phi(\mathbf{r}) = \text{const}$. However, in the continuum, the effective gauge field can be defined in space by the modulation phase point to point; whereas in resonator lattices, it is implicitly related to the modulation phase through a line integration. One also finds that, for Bloch-wave modulations with $u(\mathbf{r})$ having the same periodicity as the static photonic crystal, $\mathbf{A}_{\text{eff}}(\mathbf{r})$ is periodic and the net effective magnetic flux through a unit cell vanishes. As we will show next, for certain Floquet photonic crystals, even though the net magnetic flux is zero through a unit cell, the Floquet bands attain nonzero Chern numbers. This represents a photonic analogue of the anomalous quantum Hall effect [25], which is distinct from the photonic analogues of the quantum Hall and quantum spin Hall effects proposed in Ref. [2] and Ref. [1], respectively.

The example of the Floquet photonic crystal we studied begins with a two-dimensional photonic crystal with a triangular lattice (lattice constant a) of dielectric rods ($r = 0.27a$) with relative permittivity $\epsilon_r = 12$ (corresponding to silicon or gallium arsenide) in a background with relative permittivity of $\epsilon_r = 2$ (corresponding to silicon dioxide) [Fig. 1(a)]. A honeycomb sublattice (lattice constant $3a$) is created inside the triangular lattice, which consists of smaller rods ($r = 0.145a$, $\epsilon_r = 12$) and holes ($r = 0.27a$, $\epsilon_r = 1$). The band structure of the TM modes calculated using the plane-wave expansion method [26] is shown in Fig. 1(b), and the out-of-plane electric field of the modes of highlighted band 2 at Γ and K points is shown in Fig. 1(c). As time-reversal symmetry is not broken in the static photonic crystal, all the bands are topologically trivial with zero Chern numbers.

Next, we introduce temporal modulations of permittivity in order to couple bands 1 and 2 in Fig. 1(b) to create

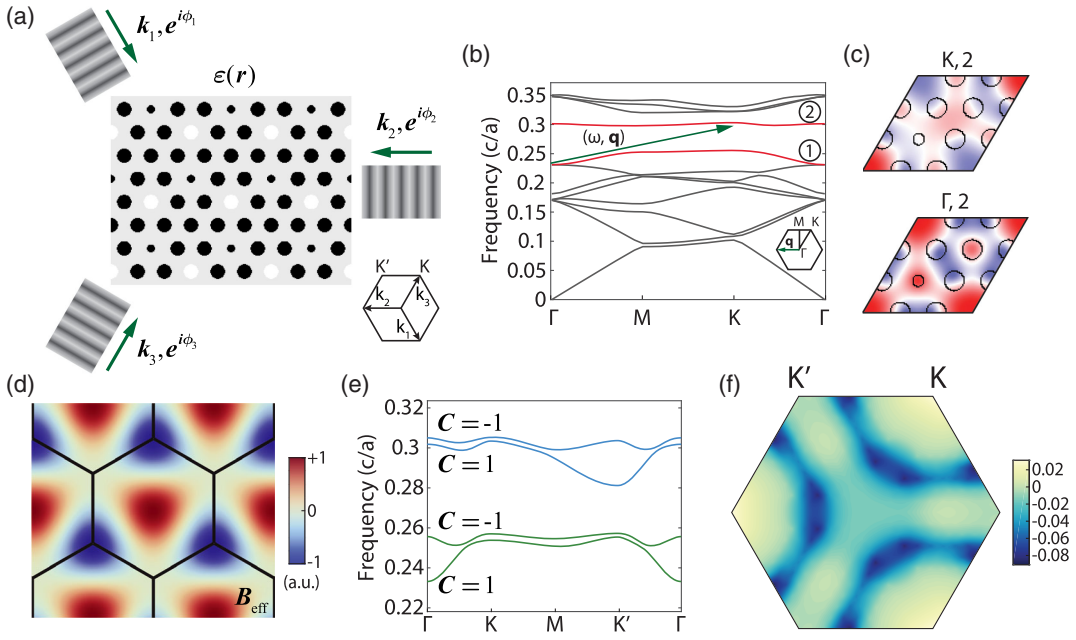

FIG. 1. Effective magnetic fields in the Floquet photonic crystal. (a) The Floquet photonic crystal consists of a static photonic crystal and the permittivity modulations of three Bloch waves with momenta equal to the three K points and phases $\phi_{1,2,3}$. Black, gray, and white areas in the static photonic crystal have relative permittivities of 12, 2, and 1, respectively. (b) Band structure of the TM modes of the static photonic crystal. The permittivity modulation with frequency ω and Bloch momentum $\mathbf{q}$ (green arrow) is used to couple the two highlighted bands (red). (c) Out-of-plane electric field in the unit cell corresponding to the modes of band 2 at Γ and K points. (d) Distribution of the effective magnetic field $\mathbf{B}_{\text{eff}}$ induced by the Bloch-wave modulations for $\phi_1 = 0$, $\phi_2 = 2\pi/3$, and $\phi_3 = 4\pi/3$. The net effective magnetic flux through the Wigner-Seitz unit cell is zero. (e) Floquet band structure of the modulated photonic crystal, which is formed from hybridization of static bands 1 and 2 of Fig. 1(b). The Chern number of each band is indicated for the modulation parameters specified in the text. (f) Berry curvature in the Brillouin zone for the top blue Floquet band in Fig. 1(e).

topologically nontrivial Floquet bands. The frequency of the modulation is slightly larger than the band gap between the two bands, and its spatial profile has the following form:

$$\delta(\mathbf{r})e^{i\phi(\mathbf{r})} = \sum_{j=1}^{3} u_j(\mathbf{r})e^{i(\mathbf{k}_j\cdot\mathbf{r}+\phi_j)}, \tag{6}$$

where $u_{1,2,3}(\mathbf{r})$ are functions with the same spatial periodicity as the static photonic crystal, and we choose the coordinate origin at the center of an air hole. The modulation of Eq. (6) is a superposition of three Bloch waves, which could lead to a rotating distribution of permittivity. For example, if we consider the case where $\mathbf{k}_{1,2,3}$ are the three equivalent K points in the Brillouin zone, with $u_{1,2,3}(\mathbf{r}) \equiv \bar{u}(\mathbf{r})$ possessing 120° rotational symmetry and $\phi_j = [2(j-1)\pi]/3$, then we have $\hat{R}_{120°}\epsilon(\mathbf{r},t) = \epsilon(\mathbf{r}, t - 2\pi/3\omega)$, where $\hat{R}_{120°}$ is the operation of 120° clockwise rotation in real space. As such, by adjusting the relative phase between the Bloch waves, we can effectively circulate the permittivity and change its chirality.

Meanwhile, because $\mathbf{k}_i - \mathbf{k}_j$ are reciprocal lattice vectors, $\delta(\mathbf{r})e^{i\phi(\mathbf{r})}$ is, by itself, of the Bloch-wave form, with a Bloch-wave vector of $\mathbf{q} = \mathbf{k}_j$, $\forall\, j$. The effective magnetic field for band 2 induced by the modulation is calculated using $\mathbf{B}_{\text{eff}}(\mathbf{r}) = \nabla \times \mathbf{A}_{\text{eff}}(\mathbf{r})$ and Eq. (5) for $\bar{u}(\mathbf{r}) \propto \epsilon(\mathbf{r})^2$ and $\phi_j = [2(j-1)\pi]/3$, which is shown in Fig. 1(d). The net magnetic flux through the Wigner-Seitz cell is zero, as expected. Figure 1(e) shows the calculated TM Floquet bands (with two repeated branches) by coupling static bands 1 and 2 with modulation parameters $\omega = 0.0491 \times 2\pi c/a$, $\phi_j = [2(j-1)\pi]/3$, and $\bar{u}(\mathbf{r}) = 0.25$ (in dielectrics) or 0 (in air). We see that K and K' points are no longer equivalent due to the momentum-carrying modulation. Although the net magnetic flux through a unit cell is zero, we find each Floquet band has a nonzero Chern number of $C = \pm 1$ [15], with the Berry curvature of one Floquet band shown in Fig. 1(f). This result represents a photonic analogue of the anomalous quantum Hall effect [25] realized in a structure beyond tight-binding models, and it indicates the existence of one-way edge modes in the Floquet band gap [27], which are truly robust against any structural defects.

We numerically demonstrate the anomalous topological edge mode through a finite-difference time-domain (FDTD) simulation using Maxwell's equation. The full simulation domain is shown in Fig. 2(a) with $a = 0.37$ μm. The boundaries of the simulation domain are composed of perfectly matched layers. The Floquet photonic crystal occupies part of the simulation domain with an edge at

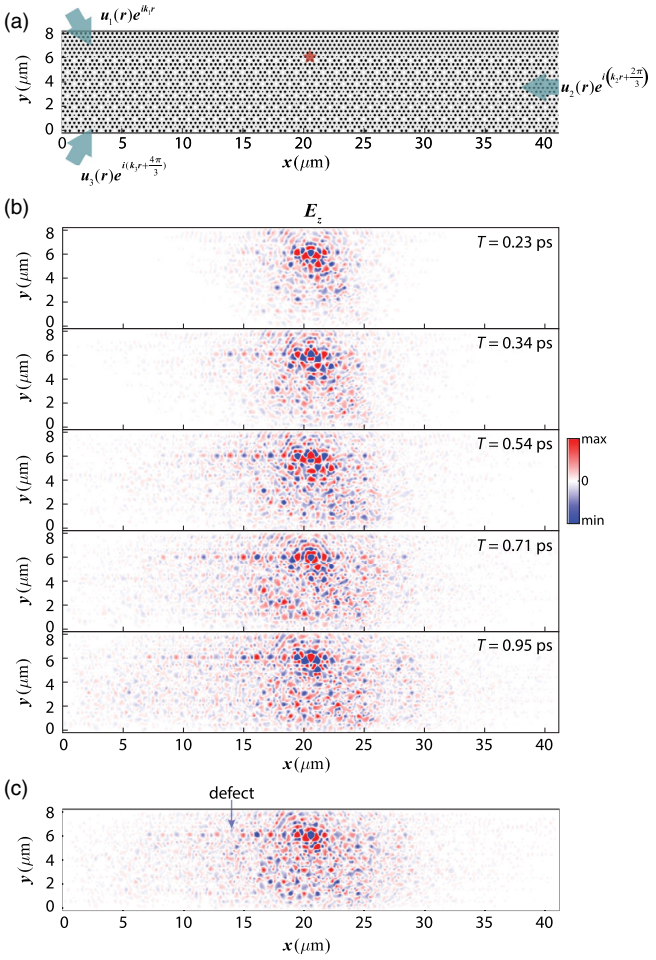

FIG. 2. Anomalous topological edge mode. (a) Full photonic structure used in the FDTD simulation with three Bloch-wave modulations with phase lagging of $2\pi/3$. The star indicates the location of the point source. (b) Propagation of the electric field E_z excited by the TM-polarized continuous-wave point source. A left-propagating one-way mode exists on the edge ($y \sim 6$ μm) of the Floquet photonic crystal. (c) Reflection immunity of the one-way edge mode in the presence of a defect. Here, the defect is created by removing a small dielectric rod on the edge.

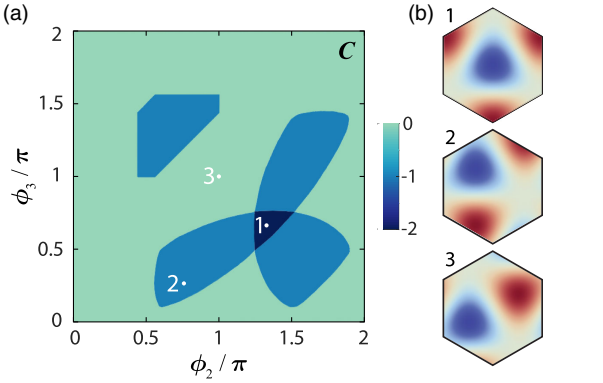

FIG. 3. Phase diagram of the Floquet photonic crystal. (a) Chern number of the higher frequency band of the Floquet two-band model for varying ϕ_2 and ϕ_3 ($\phi_1 = 0$). (b) Effective magnetic field in the Wigner-Seitz cell corresponding to the phases indicated by points 1 $(4\pi/3, 2\pi/3)$, 2 $(3\pi/4, \pi/4)$, and 3 (π, π). Figure 1(d) corresponds to point $(2\pi/3, 4\pi/3)$. For the calculation of the effective magnetic field, we used $\bar{u}(\mathbf{r}) \propto \epsilon(\mathbf{r})^2$ to remove the higher order texture due to static permittivity distribution in the photonic crystal.

$y \sim 6$ μm. The applied temporal modulation is the same as that used for the calculation of the Floquet band structure above. A TM-polarized continuous-wave point source with a frequency of $\omega_s/2\pi = 0.2549c/a = 206.7$ THz on the edge of the Floquet photonic crystal is used to excite the electromagnetic waves. The time evolution of the excited electric field is shown in Fig. 2(b), where a one-way edge mode can be clearly identified, along with bulk excitations due to the incomplete Floquet band gap, which can be optimized by further engineering of the photonic crystal and temporal modulation. When the edge mode encounters a defect, it keeps unidirectional propagation without reflection [Fig. 2(c)], which is evidence of topological protection. Note that the appearance of a one-way edge mode after the defect is not due to the reexcitation by bulk fields because of its phase coherence, whereas the bulk fields have a fluctuating phase distribution along the edge.

The topological properties of Floquet photonic crystals can be controlled by the phase of Bloch waves, which also determines the distribution of the effective magnetic field in real space. Figure 3(a) shows a phase diagram of the model above, where topologically different phases with the Chern number ranging from 0 to -2 exist. The distribution of the effective magnetic field in the Wigner-Seitz cell for a few phases is shown in Fig. 3(b). Contrary to the tight-binding model of the anomalous quantum Hall effect [25], where the sign of the Chern number is related to the chirality of the electron hopping amplitude, the sign of the Chern number in this continuum model is not directly related to the chirality of modulations (i.e., $\phi_3 > \phi_2 > \phi_1$ or $\phi_2 > \phi_3 > \phi_1$), and the two chiralities have very different Chern number distributions. We also find that, if the modulation strength is increased, a positive Chern number appears around $\phi_1 = \phi_2 = \phi_3 = 0 \mod 2\pi$ [15], which is remarkable because, intuitively, the Chern number is expected to be zero when the chirality of modulation is absent. These novel topological band features in Floquet photonic crystals are largely due to the delocalized wave interference in the continuum, and they are difficult to produce in tight-binding types of systems.

Using Bloch-wave modulations to realize dynamic beam steering and topological photonic states for which the property can be reconfigured by controlling the phase and wave vector of Bloch waves has practical significance. Bloch waves are eigenmodes of periodic structures and can be naturally excited by pumps with the frequency and wave vector that satisfy the dispersion relation. When multiple Bloch waves are used, the relative phases can be controlled

by continuously tunable phase shifters. Such Bloch-wave induced permittivity modulations can be generated through nonlinear optical effects or optomechanical interactions with optical and acoustic traveling waves, respectively. By trapping the optical or acoustic pump waves in guided resonances of photonic crystals [9–11], one can significantly enhance the modulation strength in a large area with experimentally available pump power [15]. Although, in this Letter, we considered modulation induced interband coupling, low-frequency mechanical modulations are more suitable for intraband coupling, which might also result in nontrivial Floquet bands.

In summary, we have revealed the generation of effective magnetic fields for photons in photonic crystals under continuous spatiotemporal modulations. In this paradigm, we showed a photonic analogue of an anomalous quantum Hall effect with unique topological band features due to delocalized wave interference. Other than that, a variety of combinations of spatiotemporal modulations and static photonic crystals can be explored to implement physics that otherwise seems difficult with discretely modulated resonator lattices, including those models requiring a nonreciprocal phase on beyond-nearest-neighbor couplings. For instance, the scenario when the modulations have a different periodicity than that of the static photonic crystals [e.g., when $\mathbf{k}_i - \mathbf{k}_j$ in Eq. (6) are not the primitive reciprocal lattice vectors] might be used to generate fractal photonic spectra, such as the Hofstadter butterfly [28]. Beam steering using effective gauge fields [6,29] becomes feasible in the continuum case because it avoids the mode matching issue between single-mode beams and arrays of resonators that discretely sample the beam. One could also use the modulated continuum to realize "light stopping" [30]. To that end, modulations with $\mathbf{q} = 0$ should be used in order to preserve the wave vector components of the signal pulse; then, by adiabatically tuning the modulation amplitude, the topography of the coupled Floquet bands alters (e.g., shift of band edges), causing substantial change of the group velocity of light for coherent information storage.

We are very grateful to Yu Shi and Shanhui Fan for providing the FDTD simulation code. This work is supported in part by U.S. National Science Foundation under Grant No. ECCS-1809707.

*kfang3@illinois.edu

[1] M. Hafezi, E. A. Demler, M. D. Lukin, and J. M. Taylor, Robust optical delay lines with topological protection, Nat. Phys. **7**, 907 (2011).

[2] K. Fang, Z. Yu, and S. Fan, Realizing effective magnetic field for photons by controlling the phase of dynamic modulation, Nat. Photonics **6**, 782 (2012).

[3] M. Hafezi, S. Mittal, J. Fan, A. Migdall, and J. Taylor, Imaging topological edge states in silicon photonics, Nat. Photonics **7**, 1001 (2013).

[4] Q. Lin, M. Xiao, L. Yuan, and S. Fan, Photonic Weyl point in a two-dimensional resonator lattice with a synthetic frequency dimension, Nat. Commun. **7**, 13731 (2016).

[5] L. D. Tzuang, K. Fang, P. Nussenzveig, S. Fan, and M. Lipson, Non-reciprocal phase shift induced by an effective magnetic flux for light, Nat. Photonics **8**, 701 (2014).

[6] K. Fang and S. Fan, Controlling the Flow of Light Using the Inhomogeneous Effective Gauge Field that Emerges from Dynamic Modulation, Phys. Rev. Lett. **111**, 203901 (2013).

[7] T. Kitagawa, E. Berg, M. Rudner, and E. Demler, Topological characterization of periodically driven quantum systems, Phys. Rev. B **82**, 235114 (2010).

[8] N. H. Lindner, G. Refael, and V. Galitski, Floquet topological insulator in semiconductor quantum wells, Nat. Phys. **7**, 490 (2011).

[9] J. Lee, B. Zhen, S.-L. Chua, W. Qiu, J. D. Joannopoulos, M. Soljačić, and O. Shapira, Observation and Differentiation of Unique High-q Optical Resonances near Zero Wave Vector in Macroscopic Photonic Crystal Slabs, Phys. Rev. Lett. **109**, 067401 (2012).

[10] C. W. Hsu, B. Zhen, J. Lee, S.-L. Chua, S. G. Johnson, J. D. Joannopoulos, and M. Soljačić, Observation of trapped light within the radiation continuum, Nature (London) **499**, 188 (2013).

[11] M. Zhao and K. Fang, Mechanical bound states in the continuum for macroscopic optomechanics, Opt. Express **27**, 10138 (2019).

[12] D. A. Fuhrmann, S. M. Thon, H. Kim, D. Bouwmeester, P. M. Petroff, A. Wixforth, and H. J. Krenner, Dynamic modulation of photonic crystal nanocavities using gigahertz acoustic phonons, Nat. Photonics **5**, 605 (2011).

[13] D. B. Sohn, S. Kim, and G. Bahl, Time-reversal symmetry breaking with acoustic pumping of nanophotonic circuits, Nat. Photonics **12**, 91 (2018).

[14] C. Chicone, *Ordinary Differential Equations with Applications* (Springer Science and Business Media, New York, 2006).

[15] See Supplemental Material at http://link.aps.org/supplemental/10.1103/PhysRevLett.122.233904 for the calculation of the Floquet band structure, the derivation of the effective gauge field, and the potential experimental realizations, which include Refs. [10,11,13,16–24].

[16] S. Combrié, A. De Rossi, Q. V. Tran, and H. Benisty, GaAs photonic crystal cavity with ultrahigh Q: Microwatt nonlinearity at 1.55 μm, Opt. Lett. **33**, 1908 (2008).

[17] H. Liang, R. Luo, Y. He, H. Jiang, and Q. Lin, High-quality lithium niobate photonic crystal nanocavities, Optica **4**, 1251 (2017).

[18] T. Baba, Slow light in photonic crystals, Nat. Photonics **2**, 465 (2008).

[19] J. Jin *et al.*, Topologically enabled ultra-high-Q guided resonances robust to out-of-plane scattering, arXiv:1812.00892.

[20] C. Xu, G. Wang, Z. H. Hang, J. Luo, C. T. Chan, and Y. Lai, Design of full-k-space flat bands in photonic crystals beyond the tight-binding picture, Sci. Rep. **5**, 18181 (2016).

[21] M. Notomi, E. Kuramochi, and T. Tanabe, Large-scale arrays of ultrahigh-Q coupled nanocavities, Nat. Photonics **2**, 741 (2008).

[22] K. C. Balram, M. I. Davanço, J. D. Song, and K. Srinivasan, Coherent coupling between radiofrequency, optical and acoustic waves in piezo-optomechanical circuits, Nat. Photonics **10**, 346 (2016).
[23] M. Eichenfield, J. Chan, R. M. Camacho, K. J. Vahala, and O. Painter, Optomechanical crystals, Nature (London) **462**, 78 (2009).
[24] K. Fang, J. Luo, A. Metelmann, M. H. Matheny, F. Marquardt, A. A. Clerk, and O. Painter, Generalized non-reciprocity in an optomechanical circuit via synthetic magnetism and reservoir engineering, Nat. Phys. **13**, 465 (2017).
[25] F. D. M. Haldane, Model for a Quantum Hall Effect Without Landau Levels: Condensed-Matter Realization of the "Parity Anomaly", Phys. Rev. Lett. **61**, 2015 (1988).
[26] S. G. Johnson and J. D. Joannopoulos, Block-iterative frequency-domain methods for Maxwells equations in a planewave basis, Opt. Express **8**, 173 (2001).
[27] M. S. Rudner, N. H. Lindner, E. Berg, and M. Levin, Anomalous Edge States and the Bulk-Edge Correspondence for Periodically Driven Two-Dimensional Systems, Phys. Rev. X **3**, 031005 (2013).
[28] D. R. Hofstadter, Energy levels and wave functions of Bloch electrons in rational and irrational magnetic fields, Phys. Rev. B **14**, 2239 (1976).
[29] Q. Lin and S. Fan, Light Guiding by Effective Gauge Field for Photons, Phys. Rev. X **4**, 031031 (2014).
[30] M. F. Yanik and S. Fan, Stopping Light All Optically, Phys. Rev. Lett. **92**, 083901 (2004).